# Experimental analysis and mechanical modeling of T-stubs with four bolts per row

**Latour Massimo*[1], Rizzano Gianvittorio [1], Santiago Aldina[2], Simões da Silva Luis[2]**

[1]University of Salerno, Department of Civil Engineering, mlatour@unisa.it, g.rizzano@unisa.it
[2] ISISE - University of Coimbra, Department of Civil Engineering, aldina@dec.uc.pt, luisss@dec.uc.pt

**SUMMARY**

The behaviour of steel structures is significantly affected by the connections between the steel members. For this reason, special attention to the prediction of the joints rotational behaviour is devoted by Eurocode 3 which provides the well-known component method. In EC3, starting from the results of several researches, the formulations for the characterization of the behaviour of T-stubs with two bolts per row are given, but with reference to T-stubs with four bolts per row, even though they are present in many actual structural situations, the limited number of experimental tests and analytical models has not led yet to the codification of this component in the code. In this work, starting from the results of three experimental tests on T-stub with four bolts per row, carried out at the laboratory on materials and structures of the University of Coimbra, a FE model in ABAQUS has been set up in order to analyse the yield line patterns corresponding to the different collapse mechanisms. Subsequently, with reference to the yield line shape different from that of T-stub with two bolts per row, the effective lengths have been revaluated applying an energy approach. The definition of the effective width for all the possible collapse mechanisms allowed to set up a proposal for determining the resistance of T-stubs with 4 bolts per row consistent with the approach provided by Eurocode 3. The model accuracy has been verified by means of a comparison with the results provided by a numerical analysis.

*Keywords: T-stubs, Mechanical modelling, Finite element method, Yield lines, Experimental tests, Four bolts*

**Corresponding author*

## 1. INTRODUCTION

In current practice, aiming to reduce the structural costs, performance criteria have been introduced in codes that specify the details of the structures in order to concentrate the dissipation of the energy induced by rare seismic events in specific zones (Bruneau et al., 1998; Mazzolani & Piluso, 1996; Grecea et al., 2004). In particular, it is well known that the design of steel Moment Resisting Frames (MRFs), according to EC8 (CEN, 2005b), can be carried out by locating the dissipative zones in beams or joints by means of an appropriate choice of the ratio between the flexural resistance of the beams and the bending resistance of the joints. When full strength connections are adopted, the joints are designed to be over-strength with respect to the beams, taking into account the random material variability and the steel strain-hardening (Latour & Rizzano, 2013; Piluso & Rizzano, 2007; Engelhardt et al., 1997; Simões da Silva et al., 2004). In this way, the full exploitation of the plastic hinges at beam ends is guaranteed by a bending moment lower than the joint plastic resistance. In the opposite case, i.e. when partial strength connections are adopted, the plastic zones are located in the joints and the energy dissipation supply of the frame is governed by the capacity of the connecting elements to withstand plastic excursions. In this latter case, as already stated in Iannone et al. (2011) and Simões da Silva et al. (2009), in order to guarantee a dissipative behavior of the frame, a resistance hierarchy criterion has to be applied at the level of the joint components by over strengthening the non-dissipative components and concentrating the yielding in the dissipative joint elements.

Furthermore, the rotational behavior of the beam-to-column connections is of great importance also in determining the elastic properties of MRFs. The distribution of the internal forces in the members, the lateral deformability and the dynamic properties of the frames are all characteristics related to the beam's and to the joint's stiffness. Depending on the ratio between the rotational stiffness of the joints and the flexural stiffness of the connected beams, the joints can be designed such as to behave as fully restrained, as a hinge able to transfer only the shear forces or to work as a semi-rigid joint.

In order to account for the joint stiffness and strength in structural analyses, EC3 (CEN, 2005a) provides the so-called Component Method, which is a general approach that can be used to calculate the characteristics of any type of joint, provided that all the active components are properly identified and modeled. In case of bolted connections, the main joint components responsible for the joint ductility, such as the column flange in bending, the end-plate in bending and the angles in tension are modeled by means of an equivalent T-stub in tension. In the technical literature, several experimental and modeling works deal with the characterization of the behavior of T-stubs fastened by means of two bolts (Douty & McGuire, 1965; Zoetemeijer, 1974; Zoetemeijer P., 1990; Yee & Melchers, 1986; Jaspart, 1991; Faella et al., 2000; Gutierrez et al., 2010), being the case of T-stubs with more than two bolts per row not considered, even though it is a sub-assemblage that is applied in many practical situations [Weynand & Oerder, 2013 and Borges & Bouron, 2011].

In this paper, in order to provide a contribution to improve the model given in EC3 extending it to cases not currently covered in the code, attention is focused on the experimental and theoretical analysis of T-stubs with four bolts per row covering practical cases, such as the ones illustrated in Fig. 1.

**<Fig.1>**

So far, the work mainly focuses on experimental tests carried out at the University of Coimbra, whose results have been used to set up a calibrated finite element model. Afterwards, on the base of the results of a parametric analysis carried out by means of the FE model, an analytical formulation for the prediction of the plastic resistance of T-stubs with four bolts per row is developed (Trezza, 2013).

In particular, during the experimental activity at the laboratory, three tests have been performed on specimens designed to reproduce the three typical T-stubs failure modes. On the basis of these tests, a finite element model accounting for all sources of non-linearity has been complemented in ABAQUS software and its accuracy has been verified by means of comparison with the experimental results. Subsequently, in order to carry out a complete model for the prediction of the resistance of T-stubs with four bolts in a row, the analysis of the possible yield line patterns arising in the flange plate has been developed, by applying the FE model to several cases with different bolt/plate stiffness ratio and with different values of the T-stub width. In this phase, particular attention has been devoted to the type-2 failure mechanism, which is the collapse mechanism most common. Therefore, the yield line method has been applied to all the failure modes in order to define the T-stub effective length, by following a procedure analogous to that already applied by Zoetemeijer (1974) and by Demonceau and his co-authors (2010). In particular, by equating the work done by the external load and the internal work developed along the yield lines, the effective length of the equivalent T-stub in tension has been determined for all the possible failure mechanisms. As a conclusion of the paper, a formulation able to provide the strength of a T-stub with four bolts per row, according to the approach of EC3 has been developed and its accuracy has been verified by means of a parametric analysis carried out in the ABAQUS software.

## 2. Collapse Mechanisms of T-stubs with 4 bolts per row

As already stated, the component method currently codified in EC3 is a general method for characterizing, by means of a mechanical approach, the whole behavior up to failure of steel joints. The method can be applied by following three steps (Jaspart, 1991; Faella et al., 2000):

1. Component Identification;
2. Characterization of the Joint Components;
3. Assembly of a Mechanical Model.

In EC3, one of the main components used to characterize the behavior of bolted plates, such as the column flange in bending or the extended end plate in bending, is the so-called equivalent T-stub in tension. As mentioned before, a T-stub is a structural sub-assemblage obtained by fastening two Tees through the flanges by means of two or more bolts. Its axial response is usually studied in order to model the behaviour in bending of bolted plates starting from the definition of one or more equivalent T-stubs in tension. For the last thirty years, the monotonic and cyclic behaviors of T-stubs fastened with two bolts have been extensively studied from the experimental and theoretical point of view (Douty & McGuire, 1965; Zoetemeijer, 1974; Zoetemeijer, 1990; Yee & Melchers, 1986; Jaspart, 1991; Faella et al., 2000; Gutierrez et al., 2010, Bijlaard, 2004; Latour & Rizzano, 2013; Elghazouli, 1998; Latour et al., 2011). In fact, many models able to predict monotonic (stiffness, resistance, ductility) and cyclic behavior of T-stubs fastened with two bolts are available in technical literature and, furthermore, the main rules for defining a simplified monotonic model are provided by EC3 (Bernuzzi et al., 1996; Ermopoulos & Stamatopoulos, 1996a; Girao Coelho, 2004; Girao Coelho et al., 2004; Latour & Rizzano, 2012; Nogueiro et al., 2009; Piluso & Rizzano, 2008; Clemente et al., 2005; Della Corte et al., 2002; Faella et al., 1998).

Nevertheless, in spite of the extensive study on classical T-stubs, the research of past decades has almost neglected the study of further sub-assemblages useful for the modeling of other structural situations quite common in practice. As an example, in the current version of EC3 it is not possible to model end plates with two bolt rows outside the beam flange or end-plates with more than two bolts on the same row (Fig. 1). Therefore, in order to amplify the code framework, further research efforts are still needed. In this paper, as already underlined, the T-stub with four bolts per row, which is a sub-assemblage that can be used to study some of the cases not ruled by EC3, is considered. At present time, some studies on the T-stub with four bolts per row have already been carried out by Demonceau et al. (2010, 2012) and Kozlowski & Pisarek (2008.). In both works, the basic formulas to define the resistance of the T-stubs and the effective lengths of end-plates fastened with four bolts per horizontal row have been determined.

(a) In the approach proposed by Demonceau and his co-authors (2010), in analogy with the classical T-stub theory, three failure mechanisms can arise depending on the relative resistances of plate and bolts. In case of strong bolt and weak plate, the failure arise due to the development of four plastic hinges (Mechanism type-1), two in correspondence of the flange-to-web connection and two in correspondence of the bolts closer to the T-stub web. Conversely, when the T-stub flange is strong and the bolts are weak, the collapse is due to the simultaneous failure of the four bolts (Mechanisms type-3). In the intermediate cases, the collapse is due to the failure of the bolts close to the T-stub web that attains the ultimate load after the partial development of the plastic hinges in correspondence of the flange-to-web connections (Mechanism type-2), as depicted in Fig. 2.

**<Fig.2>**

Based on these hypotheses, a simplified beam model that extends the formulations given by EC3 to the case of T-stub with four bolts in one row, has been developed by Demonceau et al. (2010). Assuming rigid-plastic behavior of the steel and elastic distribution of the forces in the bolts up to failure, the equations reported in Table 1 have been obtained.

**<Table 1>**

The symbols adopted in Table 1 have the following meanings:

- $d_w$ is the diameter of the washer;
- $e_w=d_w/4$; $\Sigma B_{t,Rd}$ is the sum of the plastic resistances of the bolts fastening the T-stub;
- $M_{pl,1,Rd} =0,25 l_{eff,1} t_f \, f_y$ is the flexural plastic moment of the plate in case of mechanism type-1, which is expressed as the product of the effective length to be used in case of mechanism type-1, of the plate thickness and of the yielding stress of the steel composing the plate;
- $M_{pl,2,Rd} =0,25 l_{eff,2} t_f \, f_y$ is the flexural plastic moment of the plate in case of mechanism type 2, which is evaluated considering the effective length arising in case of mechanism type-2;
- $l_{eff,1}$ is the minimum among the effective lengths that can arise in case of circular, non-circular and beam patterns,
- $l_{eff,2}$ is the minimum between the effective lengths that can arise in case of non-circular and beam pattern;
- $n$ is the distance of the bolt closer to the T-stub web from the free edge;
- $m$ is the distance between the bolt closer to the web and the plastic hinge arising at the flange-to-web attach, whose distance from the T-stub web is assumed, according to EC3, equal to 0.8 the root of radius in case of rolled T-stub or equal to $0.8 \cdot \sqrt{2}$ the weld throat in case of welded T-stub;
- $n_1$ is the distance between the two bolts;
- $n_2$ is the distance of the external bolt from the free edge.

The meaning of the symbols is further clarified in Fig. 3.

**<Fig.3>**

It is possible to note from the expressions given in <Table **1>**, that the equations for predicting the resistance of the 4-bolts T-stub are unchanged with respect to the classical ones in case of mechanisms of type-1 and type-3. In fact, in case of mechanism type-1 there is almost no influence of the further bolts that, being in the zone of the plate that remains undeformed, do not give any contribution to the T-stub resistance. In case of mechanism type-3, the formula is the same as the classical expression, but the resistance of the T-stub is doubled due to the additional bolts. However, in case of mechanism type-2 there are significant differences in the T-stub behavior. In fact, in this case, the further two bolts oppose to the plate uplift, significantly increasing the resistance of the T-stub. It has to be noted that the application of the equations obtained by Demonceau et al. (2010) requires the definition of appropriate effective lengths which will be the topic of discussion in the next paragraphs.

## 3. Experimental Evaluation

### *3.1 Description of the Tests*

In order to analyze the force-displacement behavior of T-stubs with four bolts per row, an experimental program composed by three tests has been performed at the laboratory on materials and structures of the University of Coimbra. The tested specimens were designed with the aim to achieve the development of each of the three typical failure modes described in the previous section. For this purpose, the geometrical characteristics of the T-stubs, such as the bolts pitch and the plate thickness, have been determined for each specimen according to the design formulas developed in (Demonceau et al., 2010). As far as the expressions of the effective lengths are not available in the design phase, the simplified hypotheses of yield lines corresponding to a beam pattern has been made.

#### *3.1.1 Material and geometrical characterization*

All T-stubs have been assembled by welding steel plates composing the web and the flange, made of S355 steel fastened through the flanges by means of four M12 bolts made of 8.8 class high strength steel (CEN, 2005c), as depicted in Fig. 4. The material properties of the plates composing the specimens have been tested in a preliminary phase by carrying out tensile coupon tests. In Fig. 5 the material behavior is shown in terms of nominal stress-strain values, true stress - logarithmic strain behavior and also a quadri-linear appropriate model that has been used in the finite element analysis (Table 3). The true stress-true strain response has been determined according to the procedure provided by RILEM (1990), while the quadri-linear approximation has been determined by equating the area under the true stress - logarithmic strain curve to the theoretical one.

**<Fig.4>**
**<Fig.5>**

In order to promote the development of the three typical failure modes, the specimens have been realized as follows:

- *Test 1: T-stub designed to achieve the development of a weak plate-strong bolt mechanism.* The specimen is composed by a 105x250x10 mm flange plate, bolt distance from the web and pitch equal to 46 mm;
- *Test 2: T-stub designed to achieve a mechanism type-2.* The specimen has the same geometry of specimen 1, but the flange plate has a thickness of 20 mm;
- *Test 3: T-stub designed to fail according to a mechanism type-3.* The specimen is composed by a flange plate of 20 mm and bolts located very close to the T-stub web in order to reduce the flexural engagement of the T-stub flange plate. In this case, the distance of the bolt from the web is of 17 mm and the pitch of 29 mm (Table 2).

**<Tab.2>**
**<Tab.3>**

### *3.1.2 Experimental layout and testing procedure*

All the tests have been executed by means of a rig machine developed at the University of Coimbra (Fig.6). The machine is composed by the assemblage of a series of steel profiles, which are used to counteract the load applied by a hydraulic cylinder. In turn, such a piston pushes on a pendular "rigid column", which is used to transfer the load to the specimen. In particular, within the experimental program, a static/dynamic hydraulic cylinder with capacity of 1000 kN and stroke of 280 mm has been used. The tested specimens have been put in the middle of the "rigid column", as reported in Fig.6, and have been connected to the testing system through twelve M20 bolts applied on the T-stub webs. In order to carry out quasi-static tests, the loads have been applied under displacement control at constant velocity of 0.02 mm/s.

**<Fig.6>**

All the specimens have been instrumented with four LVDTs located on both sides of the T-stub (D1, D2, D3 and D4 in Fig. 7), in order to measure the average value of the gap opening and the elongation of the inner bolts; additionally, three others LVDTs were used to measure parasite displacements (D5, D6 and D7 in Fig. 7).

<Fig.7>

### *3.2 Results of the Tests*

As mentioned above, the first test has been designed aiming to promote the plasticization of the plate according to a mechanism type-1. Figure 8 shows some phases of the experimental test. It can be noted that the plate of Test-1 exhibited a significant plastic engagement, with a deformed shape characterized by the development of two plastic hinges in correspondence of the T-stub web and two plastic hinges in correspondence of the bolt lines (Fig. 8).

**<Fig.8>**

The collapse of the specimen occurred at a displacement of 25 mm; premature fracture of the bolts was observed because its ultimate load was reached before the complete development of the plastic hinges on the T-stub flange plate. In this case, the failure has first concerned the inner bolts and, after a partial loss of the T-stubs resistance, also the outer bolts. As the collapse was governed by the bolts fracture, the failure of this specimen can be classified as a mechanism type-2, even though a significant plastic engagement of the T-stub flange plate has occurred. Probably, the behavior was not the expected one, due to the parasite bending moment arising in the bolts which is a phenomenon usually neglected in the design formulas.

Specimen used in Test-2 had the same geometrical configuration of the first one, made exception for the flange plate that was characterized by a thickness of 20 mm. In this case the T-stub exhibited a type-2 collapse mode, characterized by the development of a plastic hinge in correspondence of the flange-to-web connection followed by the failure of the bolts. Even in this case, the collapse first arose due to the failure of the inner bolts and, after the partial loss of the load, failure of the outer bolts was also observed (Fig.9).

**<Fig.9>**

Finally, in case of Test-3, the specimen was designed to fail according to a mechanism type-3 with a thick flange plate and a small distance of the bolts from the T-stub web. Also in this case the expected behavior was obtained. In fact, for a value of the load corresponding approximately to the sum of the resistances of the four M12 bolts in tension, the failure arose due to the fracture of the bolt shaft (Fig.10).

**<Fig.10>**

For the three specimens, Fig. 11 reports the loads measured by the load cell versus the average displacements of the gap opening recorded by the two LVDTs. It can be noted that, in agreement with the design values obtained by the equations provided in Table 1, the resistance of the three specimens increases as far as the failure mechanism shifts from type-1 to type-3.

**<Fig.11>**

## 4. Finite Element Model

### *4.1 General description of the finite element model*

In order to extend the results of the experimental campaign, a Finite Element Model has been developed in Abaqus code. The FE model has been developed with two purposes: i) the first one is to understand the yield line patterns arising in the plate for each possible failure mechanism; ii) the second one is to extend the experimental results, by carrying out a parametric analysis. In order to develop the FE model, the following steps will be necessary: geometrical definition of the elements, modeling of the materials' properties, definition of the interactions arising between the elements, definition of the boundary conditions, choice of the element type and mesh size.

The goal is to define a solid three-dimensional model. The model is constituted by four elements: the flange and web of rigid support, the tested T-stub and the bolts (Fig. 12). The geometries of such parts have been generated by means of the modeling tools available in ABAQUS.

**<Fig. 12>**

Bolt and plate materials' properties have been described by means of an elastic-plastic isotropic model. The materials constituting the web and the flange plate of the T-stub have been defined, starting from the results of the coupon tensile tests, by adopting the quadri-linear approximation reported in Fig. 5. Conversely, considering the absence of experimental data for the bolts, the model proposed by Leon and Swanson (2000) has been adopted (Fig. 13). Such a model is able to predict the bolt force-displacement curve by means of four branches: the first two describe the elastic response, the third models the bolt after the initial yielding and the fourth segment represents the bolt behavior after the plastic state up to failure. In order to provide the model with the material properties in terms of stress-strain law, the above model has been expressed in terms of true stress – logarithmic strain behavior applying the same procedure used previously for the plates (RILEM, 1990). In addition, in order to model the bolts' failure, which governs the collapse of all the tested specimens, a material ductile damage in tension with a value of the ultimate strain equal to 0.05 has been defined. It has to be underlined that the adoption of the above value of the ultimate strain does not represent a limitation to the generality of the results because the value of the bolt ultimate strain affects only the T-stub ductility while the resistance, whose reliable prediction represents the goal of the paper, is not governed by the ultimate strain. In fact, a higher or lower value of the bolts ultimate strain does not significantly change the shape of the yield line patterns arising on the T-stub flange and, as a consequence, the plastic resistance of the T-stub.

Furthermore, in order to visualize the failure zone, the element removal option in ABAQUS has been adopted. The rigid support has been modeled by adopting an infinitely elastic material with very high value of the stiffness.

Concerning the element type, in order to reduce the computational effort an 8-node linear brick with reduced integration and instability mesh control has been adopted (C3D8R). In case of eight node bricks, the integration points are reduced from eight to one leading to a much lighter model. This choice does not reduce the accuracy of the analysis, provided that an instability mesh control is simultaneously applied. In fact, reduced integration elements can exhibit some kind of mesh instability such as the hourglassing (Kosloff & Frazie, 1978), which is a special case of the phenomenon known in finite elements as kinematic modes or spurious zero-energy modes. Practically, since the elements have only one integration point, it is possible for them to distort in such a way that the strains calculated at the integration point are all zero, leading to the uncontrolled distortion of the mesh. In order to avoid this phenomenon the viscous approach of ABAQUS code has been employed in the FE modeling.

The mesh size has been defined by carrying out a sensitivity analysis in the preliminary phase, by accounting also for the existing guidelines on the topic. In particular, in the work of Hongxia and her co-authors (2008) a detailed discussion is reported. In case of bolted connections the following mesh size effects have to be preliminarily evaluated: number of elements through the thickness of the flange, mesh size of the bolt and number of elements to be introduced in the contact zone. Therefore, in order to obtain accurate results the following meshing procedures have been respected: the T-stub flange plate has been meshed with a minimum size of the elements of 5 mm and at least two elements within the thickness of the plate; the rigid and strong plate of the support has been meshed with elements with maximum size of 15 mm; the bolts, which govern the collapse of the T-stubs, have been meshed with a very detailed mesh with minimum size of 2 mm (Fig. 14). Furthermore, all the parts have been partitioned in order to allow the definition of structured meshing techniques, leading in this way to stable results and good convergence of the model.

**<Fig.13>**

The interaction among the various elements has been defined according to a surface-to-surface formulation with finite sliding. In the normal direction a "hard contact" has been used, while in the tangential direction a friction coefficient equal to 0.2 has been adopted. The following interactions have been introduced in the model: interaction between the T-stub lower face and the rigid support upper face, interaction between the bolt heads and the plates' external surfaces and interactions between the bolts' shaft and the inner part of the holes on the plates.

**<Fig.14>**

In order to reduce the computational time, half specimen has been modelled accounting for the symmetry. Therefore, the back of the T-stub web plates have been restrained with a symmetry constraint, the base of the web has been fully restrained and the displacement has been imposed on the top of the T-stub. The FE model has been analyzed by means of a static non-linear analysis. In order to grasp the effect of geometric non linearity at large displacements also second order effects have been accounted for.

### *4.2 Calibration of the FEM with the experimental results*

In Figs. 15-16 the results of the FE analysis are reported both in terms of stress and yield state at failure and in terms of Force-Displacement curve. With reference to Test-1, it is possible to appreciate from Fig. 15 the accuracy of the FE model in reproducing the behavior of the specimen both in terms of force-displacement curve and in terms of deformed shape. From the results provided by the FE model the behavior of the T-stub until the collapse is provided; as expected, in case of failure going towards a mechanism type-1, the external bolt is almost ineffective, as far as it does not elongate up to the failure as observed in the inner bolt. It is also possible to note from Fig. 15 that the ductility supply and the failure branch of the experimental curve are accurately predicted by the model due to the introduction of the ductile damage in the bolt constitutive law.

**<Fig.15>**

From the FE results of Test-2 reported in Fig. 16, it is possible to note the significant behavioral difference with respect to the previous case. In fact, in this case, it is possible to clearly see the formation of only one plastic hinge in the plate with a deformed shape that gives rise to the participation of both the internal and external bolt.

The comparison with the pictures taken during the experimental tests (Fig.9) confirms that also in this case the deformed shape is faithfully reproduced. Furthermore, also the comparison with the experimental results in terms of force-displacement curve shows that the developed FE model is able to reproduce the whole curve up to failure.

**<Fig.16>**

In case of Test-3, the FE simulation, according to the experimental results, shows a clear detachment of the plate and the progressive failure of the bolts which are both called, almost in the same way, to resist to the plate uplift. Also in this case, the predictions given by the model compared with the experimental results appear sufficiently accurate (Fig. 17).

**<Fig.17>**

### *4.3 Evaluation of the yield lines families*

As already underlined in previous sections, the equations derived (Demonceau et al., 2010) for predicting the resistance of a T-stub with four bolts per row require the knowledge of the plastic resistances of the plate $M_{pl1,Rd}$ and $M_{pl2,Rd}$. According to the classical approach, $M_{pl1,Rd}$ and $M_{pl2,Rd}$ can be obtained by defining appropriate values of the equivalent effective widths, which are the parameters accounting for all the possible yield line mechanism of the T-stub flange plate. The effective width of a T-stub is a theoretical parameter that can be computed by establishing an equivalence, at the collapse condition, between the resistance of the T-stub evaluated by means of a beam model, and the resistance of the T-stub evaluated accounting for the actual yield line pattern arising in the flange plate and leading to the formation of a kinematic mechanism.

According to the classical T-stub theory, three yield line patterns can arise in the flange plate: beam pattern, non-circular pattern and circular pattern (CEN 2005a and Faella et al., 2000). Circular patterns consider the case of failure of the flange plate due to the localized action of the bolt. This yield line pattern, according to EC3, can arise only in case of mechanism type-1. In fact, in case of mechanism type-2, it can be assumed that the development of a circular pattern is not possible due to the significant prying effects acting on the T-stub flange plate (Ivanyi & Baniotopoulos, 2000). Beam patterns usually develop when the T-stub has a small width and, consequently, the deformed shape is not affected by three-dimensional effects. Conversely, non-circular patterns occur more often in case of wide T-stubs, where the deformed shape of the plate is affected by significant three dimensional effects (Fig. 18).

**<Fig.18>**

To clarify, the expressions provided by EC3 defining the effective widths of a T-stub with two bolts are here reported:

$$l_{eff,cp} = 2\pi m \quad (1)$$

$$l_{eff,np} = 4m + 1{,}25n \quad (2)$$

$$l_{eff,bp} = b \quad (3)$$

From the theoretical point of view, the definition of the effective lengths for all the possible cases can be carried out by means of the yield line method, which is an application of the kinematic theorem of the plastic collapse to bi-dimensional structures (Save et al., 1997). Referring to the circular pattern, the value of the effective width can be obtained by equating the failure load of a circular plate centrically loaded by a force with the resistance given by the beam model. Concerning the expression of the effective width corresponding to non-circular pattern, the value proposed by EC3 is a simplification of a more complex model developed by Zoetemeijer (1974). Assuming the yield line patterns represented in Fig. 19, the following expressions of the effective lengths have been proposed for mechanisms type-1 and type-2 (Zoetemeijer, 1974):

$$l_{eff1,np} = 4m + 1{,}25n \quad (4)$$

$$l_{eff2,np} = 5{,}5m + 4n \quad (5)$$

It is worth noting that in the original work of Zoetemeijer, 1974, the effective lengths are provided as a function of the prying forces, which results in a definition complicated for the application in practical design. Therefore, in order to allow a unitary and simple approach, the author proposed the adoption of a common value of the effective length equal to $l_{eff1,np}$, to be adopted both for mechanism type-1 and type-2. As demonstrated by Zoetemeijer, 1974, the main advantage of this assumption is that the results are always on the safe side and, in addition, they show a satisfactory agreement with the experimental values. This proposal is also reflected in Eurocode 3 where, as a simplification, the effective length of a T-stub is defined with a unique expression provided by Eq.4.

**<Fig.19>**

It is clear that, according to the traditional approach, aiming to carry out a model for evaluating the resistance of T-stubs with four bolts per row, it is necessary to understand *a priori* the shape of the yield line patterns arising in the flange plate for all the typical failure mechanisms.

A yield line pattern can be defined starting from the experimental observation or using advanced approaches such as the FE modeling. In this work the model developed in ABAQUS software is used in order to generate several cases with different geometries, in which the yield line pattern can be clearly recognized. To this scope, in order to point out the different shapes of the yield line patterns of four-bolts T-stub with respect to the classical yield line patterns, a direct comparison is carried out by generating several FE models with different geometry once with two-bolts and once with four-bolts. Fig. 20 reproduces the results of the developed models for all the possible yield line patterns both in case of two bolts and four bolts T-stub.

**<Fig.20>**

For mechanism type-1 it is possible to note that for all the three possible yield line patterns, as far as the second bolt row is ineffective, the failure mechanisms have no substantial differences with respect to the classical ones. Therefore, it is evident that in case of mechanism type-1 the model reported in EC3, developed in (Zoetemeijer, 1974), can be still applied neglecting the external bolts. However, some differences arise in case of mechanism type-2. While the beam pattern is still unchanged, the kinematic mechanism in case of non-circular pattern is substantially different. In fact, in such a case, the external bolt row forces the yield lines to pass through the bolts leading to a shape more similar to the non-circular pattern of Mechanism type-1. Consequently, from the observation of the FE model results it is clear that in case of 4-bolts T-stubs, a recalibration of the classical model is needed. In the next paragraphs, starting from the yield line patterns derived from the FE simulations (Fig. 20), a new analytical formulation defining the effective length is developed. In particular, the value of the effective width will be defined by means of the yield line method, starting from the knowledge of the yield line shape.

## 5 Analytical Model

In the yield line models, the deformed configuration of a plate is represented by a set of plastic hinges arising on straight lines or curves which divides the plate in planar regions able to rotate relatively. Within this approach, the elastic deformations are neglected with respect to the plastic ones and, along the yield line it is assumed that the plastic moment of the plate is reached (Save et al., 1997).

The study of the yield line models can be carried out by employing the virtual work principle. In this way, the value of the collapse load corresponding to a fixed configuration of the yield line pattern can be obtained by equating the work done by the external loads to the work developed by the yield lines. For the considered case, the first one is expressed as the product of the external load acting on the T-stub web multiplied by the corresponding displacement. Conversely, the internal work is expressed as the value of the plate plastic flexural resistance multiplied by the yield line rotation. The yield line method develops through the following steps:

1. Individuation of a possible yield line pattern;
2. Definition of the parameters characterizing the shape of the yield line family;
3. Evaluation for each yield line of the rotation due to an assigned value of the external displacement;
4. Evaluation of internal and external work;
5. Minimization of the energy dissipated by the yield lines in order to find the value of the collapse load.

It is important to underline two features of the yield line method. The first one is that the choice of the yield line pattern is not trivial and, in general, it is possible to define infinite admissible kinematic mechanisms. The second one is that, as far as it is an upper bound method, according to the static theorem of plastic collapse, among all the hypothesized kinematic mechanisms the one with the minimum collapse load gives the solution more close to the true collapse load. Therefore, by following the procedure previously reported, the collapse load could be determined for a number of yield line mechanisms evaluating the minimum value which is the closest to the true collapse load. In this work, in order to reduce the computational effort, the finite element models previously reported have been used to determine the shape of the yield lines starting from the results of the FE analysis. From the results of the analysis described in section 4.1, as already underlined, it has been realized that, in case of T-stub with four bolts per row, the only yield line pattern that cannot be modeled by means of the classical theory (Zoetemeijer, 1974) is the mechanism type-2 with non-circular pattern. As a result, for this case, the yield line method is applied by assuming the distribution of the yield lines deriving from the FE simulation, as depicted in Fig. 21.

**<Fig.21>**

The assigned pattern is characterized by two parameters: the angles $\alpha$ and $\beta$. Therefore, in order to define the internal work done by the plastic hinges, the length of the yield lines and the rotations induced by an assigned uplift $\Delta\delta_{max}$ of the plate have to be determined. The obtained results are reported in the following, indicating with $\Delta\delta$ the inner bolt elongation, with $l$ and $\theta$ the length and the rotation of the yield line, respectively:

*Yield line 1:*

$$l_1 = p + 2m \tan\alpha \tag{6}$$

$$\theta_1 = \frac{\Delta\delta}{n} \tag{7}$$

*Yield line 2:*

$$l_2 = \frac{2(m+n)}{sin\beta} \tag{8}$$

$$\theta_2 = \frac{\Delta\delta cos\alpha}{ncos(\beta-\alpha)} \tag{9}$$

*Yield line 3:*

$$l_3 = \frac{2m}{cos\alpha} \tag{10}$$

$$\theta_3 = \Delta\delta \cdot \frac{msen^2\alpha}{n} \cdot \left(\frac{1}{m\sin\alpha\tan\alpha\cot(\beta-\alpha)} - \frac{1}{m\sin\alpha}\right) \tag{11}$$

*Yield line 4:*

$$l_4 = \sqrt{n^2 + \left[m \tan \alpha + \frac{(m+n)}{tan\beta}\right]^2} \tag{12}$$

$$\theta_4 = \frac{\theta_5}{\sin{(90° - \alpha + \gamma)}} sin\alpha \tag{13}$$

*Yield line 5:*

$$l_5 = 2n \tag{14}$$

$$\theta_5 = \frac{\Delta\delta(\frac{m+n}{n})}{b} \tag{15}$$

Therefore, by equating external and internal works:

$$T(m+n) = \sum_{i=1}^{5} m_{pl,Rd}\, l_i\theta_i + \sum B_{Rd}n \tag{16}$$

where $m_{pl,Rd}$ is the flexural plastic resistance per unit of length of the plate, $T$ is the external force acting on the T-stub and $B_{Rd}$ is the bolt plastic resistance. It is evident that finding the minimum collapse load $T$ means minimizing the right hand side of Eq.(16) and in particular, as far as the bolts resistance does not depend on parameters $\alpha$ and $\beta$ it means minimizing the work done by the plastic hinges $\sum_{i=1}^{5} m_{pl,Rd}\, l_i\theta_i$. In this work, in order to obtain the value of the minimum collapse load, the effective length has been determined numerically by developing a user routine in the software Mathematica 5.1. The developed routine determines for an assigned couple of values of *m* and *n* the values of $\alpha$ and $\beta$ minimizing the energy expressed by Eq. (16) and, afterwards, the value of the effective length equal to $l_{eff} = \sum_{i=1}^{5} l_i\theta_i$. A total of 10.000 combinations of values *m* and *n* varying in the range from 10 mm to 1000 mm have been generated. From the obtained results, by means of a multiple regression analysis of the data, the following expression of the effective width has been obtained with correlation coefficient $R^2$ equal to 0.99:

$$l_{eff2,np} = 5{,}685m + 5.867n \tag{17}$$

Based on these results, the authors' proposal is to define the resistance of the T-stub with four bolts per row by adopting the formulas reported in **<Table 1>** (Demonceau et al. 2010) and the values of the effective lengths given by Eqs.(1)-(3)-(4)-(17).

## 6. Parametric Analysis and Model Accuracy

In order to check the accuracy of the proposed model for the prediction of the resistance of T-stubs with four bolts in one row, a parametric analysis has been developed in ABAQUS by employing the FE model described in Section 4. The analysis has been carried out by generating a sample of cases with different geometrical characteristics. Twenty-four models have been defined, twelve of them with a wide flange (1200 mm width) and the other twelve with a narrow flange (200 mm) (Fig. 22). The first group of models has been defined aiming to promote the development of non-circular patterns, while the second group has been defined aiming to promote the development of beam patterns. For each group the following combinations of $m$, $n_1$ and $n_2$ have been stated:

1. $m$ = 40 mm; $n_1$= 80 mm; $n_2$=35 mm
2. $m$ = 60 mm; $n_1$= 60 mm; $n_2$=35 mm
3. $m$ = 40 mm; $n_1$= 60 mm; $n_2$=55 mm

**<Fig.22>**

In addition, for each combination of $m$, $n_1$ e $n_2$, in order to develop collapses belonging to all the possible failure mechanisms, four values of the thickness have been considered: 5 mm, 10 mm, 15 mm e 20 mm. The steel grade composing the plates is S355 and the bolts are M12, 8.8 class.

The analysis has been performed with reference to half model accounting for the symmetry condition and reducing the computational effort. In Fig. 23 some of the obtained results are reported.

**<Fig.23>**

In order to compare the value obtained with the analytical model defined in previous section and results coming from the parametric analysis, it is necessary to define the plastic resistance for the T-stubs modeled in ABAQUS. To this scope, it is assumed that the model provided by EC3 considers a value of the plastic resistance corresponding to the knee of the force-displacement curve of the T-stub, which can be determined as a value 1.5 times greater than the resistance corresponding to the yielding (CEN, 2005a).

In Table   the comparison between the numerical and analytical values is therefore reported. In the table, being the geometrical parameters considered together with the values of the effective width, the collapse mechanisms type and the resulting yield line pattern are shown. It can be observed that the prediction provided by the model appears sufficiently accurate with an average value of the Model/FEM ratio equal to 1.078 and a standard deviation equal to 0.19. It is useful to observe that in the cases in which the mechanism is type-2 and the yield line pattern is non-linear, the adoption of Eq.(2) provided by EC3 leads to a substantial underestimation of the T-stub plastic resistance. In fact, the average value of the Model/FEM ratio provided by the cases in which the mechanism type-2 with non-linear yield line pattern arises, is equal to 0.74. On the sample investigated, the developed model seems to give sufficiently accurate results.

**<Tab.4>**

## 7 Conclusions

In this work, the results of a theoretical and experimental analysis dealing with the prediction of the plastic resistance of T-stubs with four bolts per row have been developed. The main results of the work could be summarized as follows:

- within the experimental analysis on three T-stubs with four bolts, the typical collapse mechanisms have been evidenced, showing that, as in the classical theory, the behaviour of the T-stub is governed by the relative resistance between the bolt and the plate. The mechanism most affected by the introduction of the external bolt row is the mechanism type-2. In addition, in case of Test-1, which exhibited a failure mode going toward mechanism type-1, a small participation of the external bolt has been evidenced. As a consequence, the experimental results have shown that in mechanism type-1 the outer bolt row can be neglected;
- the FE model developed in ABAQUS software has allowed to perform a parametric analysis and to individuate, by generating several cases with different plate/bolt resistance ratio, the differences arising in terms of yield lines between the T-stub with two and four bolts per row. The analysis has pointed out that the only yield line pattern significantly affected by the external bolt row, is the non-circular one;
- by means of a theoretical approach based on the yield line method, a model for the prediction of the T-stub plastic resistance has been proposed providing, in

particular, a new relationship for the effective length to be used in case of mechanism type 2;

- the results provided by the parametric analysis generated in ABAQUS have shown that the proposed model is able to predict the T-stub resistance with a sufficient accuracy. An average value equal to 1.078 and a standard deviation equal to 0.19 is specifically provided by the ratio Model/FEM, showing a small overestimation of this model.


## Acknowledgements

The authors acknowledge financial support of the Portuguese Foundation for Science and Technology (FCT) under research projects PTDC/ECM/110807/2009 and PTDC/ECM/116904/2010.


## References


Bernuzzi, C., Zandonini, R. & Zanon, P., 1996. Experimental analysis and modelling of semi-rigid steel joints under cyclic reversal loading. *Journal of Constructional Steel Research*, 2, pp.95-123.

Bijlaard, F., 2004. Joints in steel structures based on Eurocode 3. In *Steel & Composite Structures (ICSCS'04)*. Yuseong, Korea, 2004. Techno-Press. (TUD).

Borges, L. & Bouron, S., 2011. Verification automatisee d'assemblages metalliques. *Tracés*, 3. pp.12-16 (in french).

Bruneau, M., Uang, C.M. & Whittaker, A., 1998. *Ductile Design of Steel Structures*. U.S.A.: McGraw-Hill.

CEN, 2005a. Eurocode 3: Design of steel structures - Part 1-8: Design of joints. European Committee for Standardization, CEN, Brussels.

CEN, 2005b. Eurocode 8: Design of structures for earthquake resistance - Part 1: General rules, seismic actions and rules for buildings. European Committee for Standardization, CEN, Brussels.

CEN, 2005c. Eurocode 3: Design of steel structures - Part 1-1: General rules and rules for buildings. European Committee for Standardization, CEN, Brussels.

Clemente, I., Noè, S. & Rassati, G.A., 2005. Experimental and Numerical Analysis of the Cyclic Behaviour of T-stub Components. In *Proceedings of XX CTA Conference*. Ischia, 2005.

Demonceau, J., Jaspart, J., Muller, C. & Weinand, K., 2010. Application of Eurocode 3 to Steel Connections with Four Bolts per Horizontal Row. In SDSS', ed. *Colloquium on Stability and Ductility of Steel Structures*. Rio de Janeiro, 2010.

Demonceau, J., Oerder, R. & Weinand, K., 2012. Resistance Tables for Standardized Joints in accordance with EN1993-1-8. In *CONNECTIONS VII*. Timisoara, 2012. .

Douty, T. & McGuire, W., 1965. High Strength Bolted Moment Connections. *Journal of the Structural Division*, 91(ST2), pp.101-28.

Elghazouli, A.Y., 1998. Seismic Design of Steel Frames with Partial Strength Connections. In *Proceedings of the 6th SECED Conference on Seismic Design Practice*. Oxford, UK, 1998.

Engelhardt, M.D., Winneberger, T., Zekany, A.J. & Potyraj, T.J., 1997. Experimental investigation of dogbone moment connections. In *Proceedings of National Steel Construction Conference*. Chicago, 1997. AISC.

Ermopoulos, J. & Stamatopoulos, G., 1996a. Analytical Modeling of Column Base Plates under Cyclic Loading. *Journal of Constructional Steel Research*, 40(3), pp.225-38.

Faella, C., Piluso, V. & Rizzano, G., 1998. Cyclic Behaviour of Bolted Joint Components. *Journal of Constructional Steel Research*, 46.

Faella, C., Piluso, V. & Rizzano, G., 2000. *Structural Steel Semi-Rigid Connections*. Boca Raton: CRC Press.

Girao Coelho, A., 2004. *Characterization of the Ductility of Bolted End Plate Beam-to-Column Steel Connections*. Coimbra: Universidade de Coimbra.

Girao Coelho, A.M., Bijlaard, F. & Simoes Da Silva, L., 2004. Experimental Assessment of the Ductility of Extended End Plate Connections. *Engineering Structures*, 26, pp.1185-206.

Grecea, D., Dinu, F. & Dubina, D., 2004. Performance Criteria for MR Steel Frames in Seismic Zones. *Journal of Constructional Steel Research*, 60, pp.739-49.

Gutierrez, R., Loureiro, A., Moreno, A. & Reinosa, J.M., 2010. Axial Stiffness Prediction of non-preloaded T-stubs: an analytical frame approach. *Journal of Constructional Steel Research*, 66, pp.1516-22.

Hongxia, Y., Davison, J., Plank, R. & Burgess, I., 2008. Numerical Simulation of Bolted Steel Connections in Fire using Explicit Dynamic Analysis. *Journal of Constructional Steel Research*, 64(5), pp.515-25.

Iannone, F., Latour, M., Piluso, V. & Rizzano, G., 2011. Experimental Analysis of Bolted Steel Beam-to-Column Connections: Component Identification. *Journal of Earthquake Engineering*, 15(2), pp.214-44.

Ivanyi, M. & Baniotopoulos, C.C., 2000. *Semi-Rigid Joints in Structural Steelwork*. Springer.

Jaspart , J., 1997. *Contributions ro Recent Advances in the Field of Steel Joints, Column Baes and further Configurations of Beam-to-Column Joints and Beam Splices*. Aggregation Thesis. Liege: University of Liege.

Jaspart, J.P., 1991. *Etude de la semi-rigidite des noeuds Poutre-Colonne et son influence sur la resistance et la stabilite des ossature en acier*. PhD Tesis ed. Liege: University of Liege, Belgium.

Jaspart, J., Wald, F., Weynand, K. & Gresnigt, N., 2008. Steel Column Base Classification. *HERON*, 53(1-2).

Kozlowski, A. and Pisarek, Z. 2008. Resistance and stiffness of T-stub with four bolts. Archives of Civil Engineering, 54 (1), pp. 167-191.

Kosloff, D. & Frazie, G.A., 1978. Treatment of Hourglass patterns in low order finite element codes. *International Journal for Numerical and Analytical Methods in Geomechanics*, 2, pp.57-72.

Latour, M., Piluso, V. & Rizzano , G., 2011. Cyclic Modeling of Bolted Beam-to-Column Connections: Component Approach. *Journal of Earthquake Engineering*, 15(4), pp.537-63.

Latour, M. & Rizzano, G., 2012. Experimental Behavior and Mechanical Modeling of Dissipative T-Stub Connections. *Journal of Structural Engineering*, 138(2), pp.170-82.

Latour, M. & Rizzano, G., 2013. A Theoretical Model for Predicting the Rotational Capacity of Steel Base Joints. *Journal of Constructional Steel Research*, 91, pp.89-99.

Latour, M. & Rizzano, G., 2013. Full Strength Design of Column Base Connections accounting for Random Material Variability. *Engineering Structures*, 48, pp.458-71.

Leon, R. & Swanson, J.A., 2000. Bolted Steel Connections: tests on T-stub components. *Journal of Structural Engineering*, ( ), p. .

Mazzolani, F. & Piluso, V., 1996. *Theory and Design of Seismic Resistant Steel Frames*. London: E & FN Spon, an Imprint of Chapman & Hall.

Nogueiro, P., Simoes da Silva, L., Bento, R. & Simoes , R., 2009. Calibration of Model Parameters for the Cyclic Response of End-Plate Beam-to-Column Steel-Concrete Composite Joints. *Journal of Steel and Composites Structures*, 9(1), pp.35-58.

Piluso, V. & Rizzano, G., 2007. Random Material Variability effects on Full-strength end-plate Beam-to-Column Joints. *Journal of Constructional Steel Research*, 63(5), pp.658-66.

Piluso, V. & Rizzano, G., 2008. Experimental Analysis and modelling of bolted T-stubs under cyclic loads. *Journal of Constructional Steel Research*, 64, pp.655-69.

RILEM, 1990. Draft Recommendation - Tension Testing of Metallic Structural Materials for Determining Stress-Strain Relations under Monotonic and Uniaxial Tensile Loading. *Material and Structures*, 23, pp.35-46.

Save, G. , Massonnet, C.E., De Saxcè, G., 1997. Plastic Limit Analysis of Plates, shells and disks. *North Holland series in Applied Mathematics and Mechanics*, 43, pp.71-82.

Simões da Silva, L., Gervásio, H. and Borges, L., 2004. Reliability assessment of the post-limit stiffness and ductility of steel joints. *Journal of Constructional Steel Research,* 60(4), pp. 635-648.

Simões da Silva, L., Rebelo, C. and Mota, L. 2009. Extension of the component method to end-plate beam-to-column steel joints subjected to seismic loading, The Twelfth International Conference on Civil, Structural and Environmental Engineering Computing, Madeira, September. pp. 149-167.

Trezza, S., 2013. *Previsione del comportamento ultimo di T-stub con 4 bulloni per fila: analisi teorico-sperimentale*. Master Thesis, University of Salerno.

Weynand, K.; Oerder, R., 2013. "Typisierte Anschlüsse im Stahlhochbau", 3rd edition, Stahlbau Verlags- und Service GmbH, Düsseldorf.

Yee, Y.L. & Melchers, R.E., 1986. Moment-Rotation Curves for Bolted Connections. *Journal of Structural Engineering ASCE*, 112, pp.615-35.

Zoetemeijer P., 1990. *Summary of the Research on Bolted Beam-to-Column Connections*. Report 25-6-90. Delft: Sevin Laboratory - Steel Structures Delft University of Technology.

Zoetemeijer, P., 1974. A Design Method for the Tension Side of Statically Loaded, Bolted beam-to-column Connections. *Heron*, 20, pp.1-59.

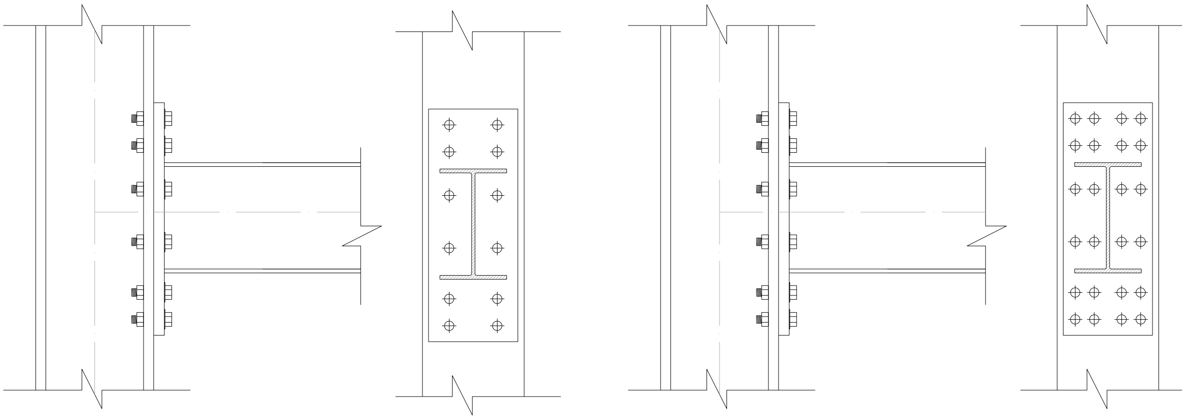

*(a) Joint configuration with T-stubs with four bolts in one row only on the extended part of the end plate*

*(b) Joint configuration with T-stubs with four bolts in one row on the extended part of the end plate, on the internal part of the end plate and on the column flange*

**Fig. 1**– Extended end-plate joint configurations with four bolts per row

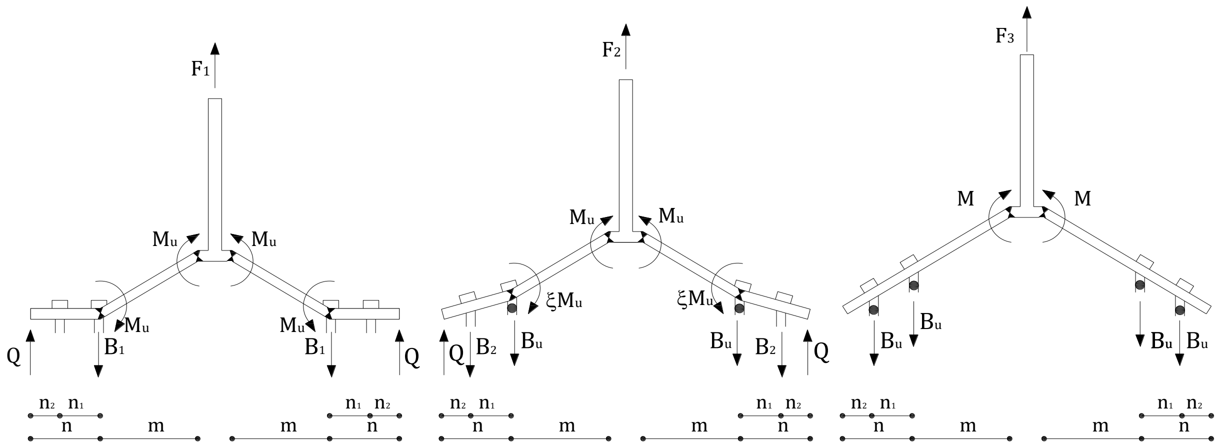


(a) Mechanism type-1

(b) Mechanism type-2

(c) Mechanism type-3

**Fig. 2**– Failure mechanisms of a T-stub with four bolts in one row

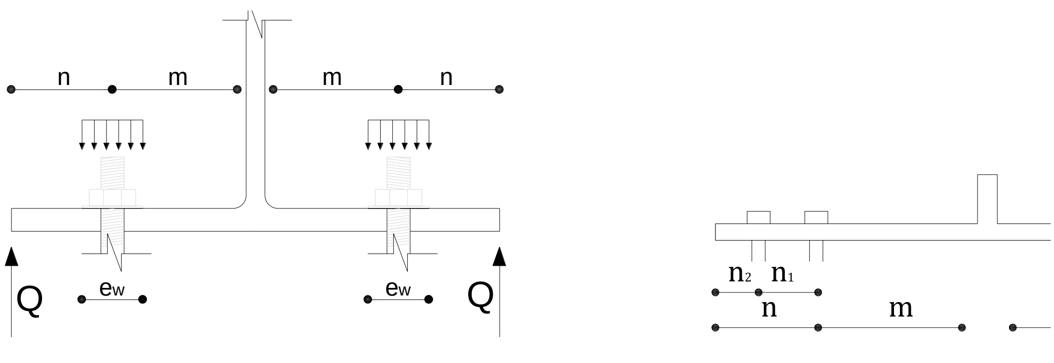


**Fig. 3**– T-stub geometrical properties

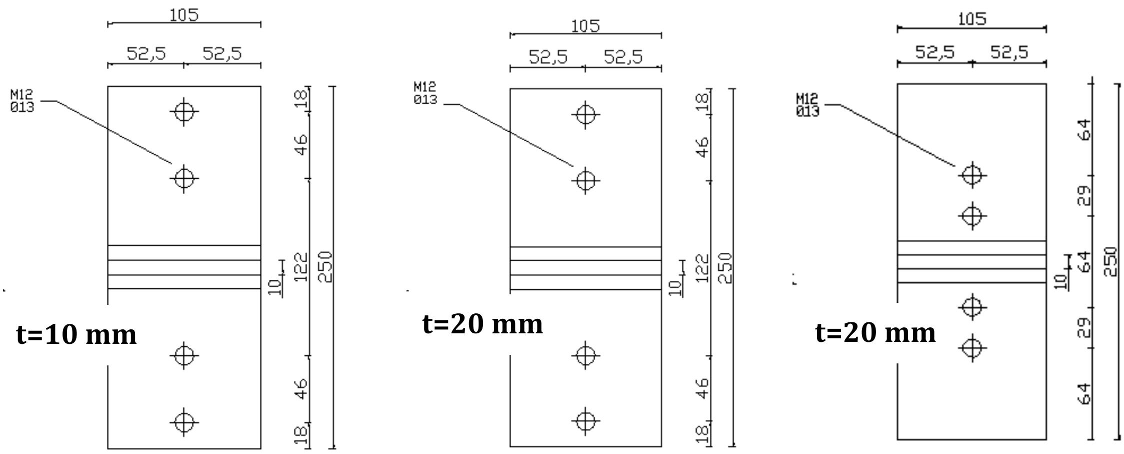


**Fig. 4** – Tested Specimens

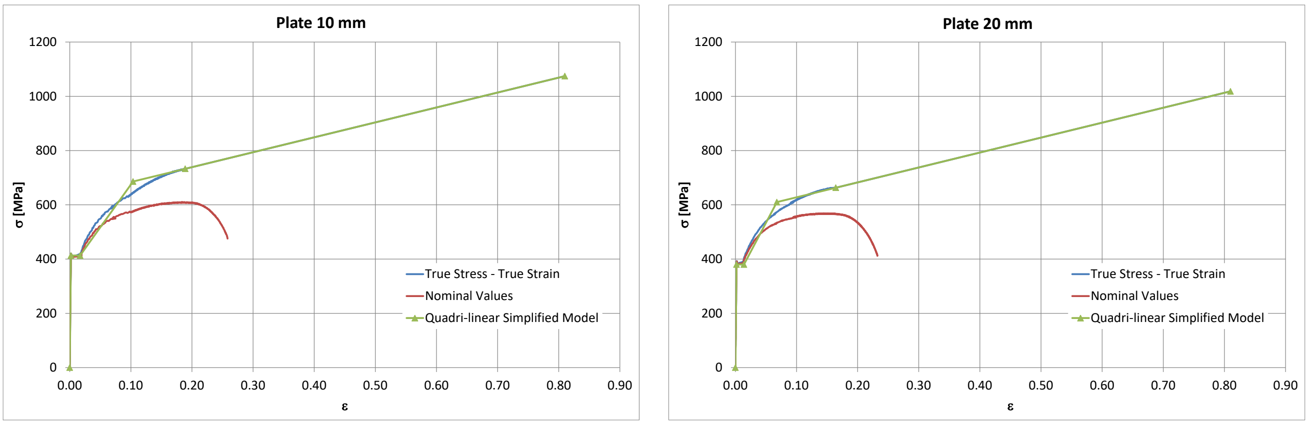


**a)** Plate $t_f$=10mm **b)** Plate $t_f$=20mm

**Fig. 5**– Results of the tensile tests on the materials composing the plate

a)

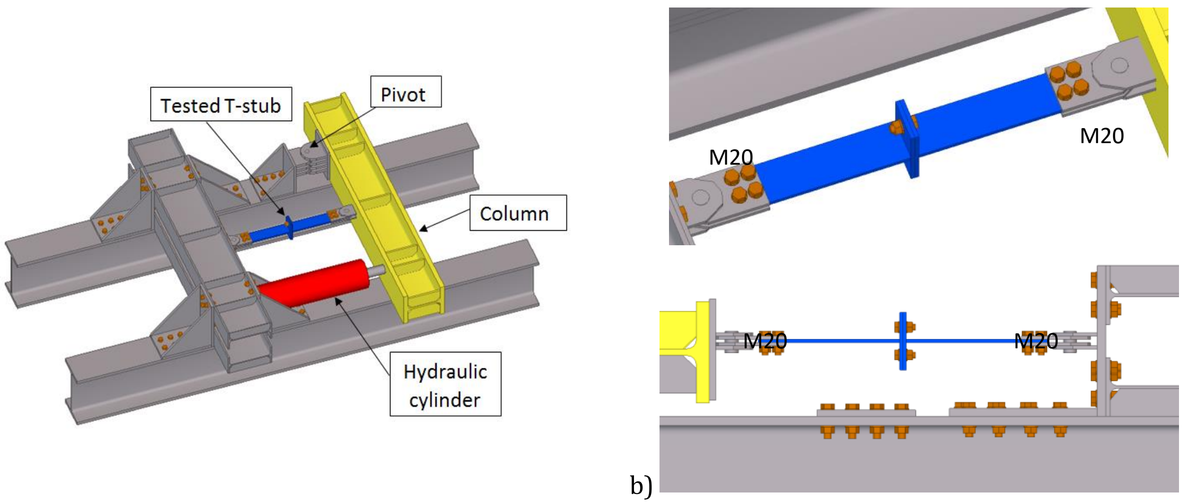


b)

**Fig.6** – Experimental Layout: a) general view; b) detailed views of the tested T-stub.

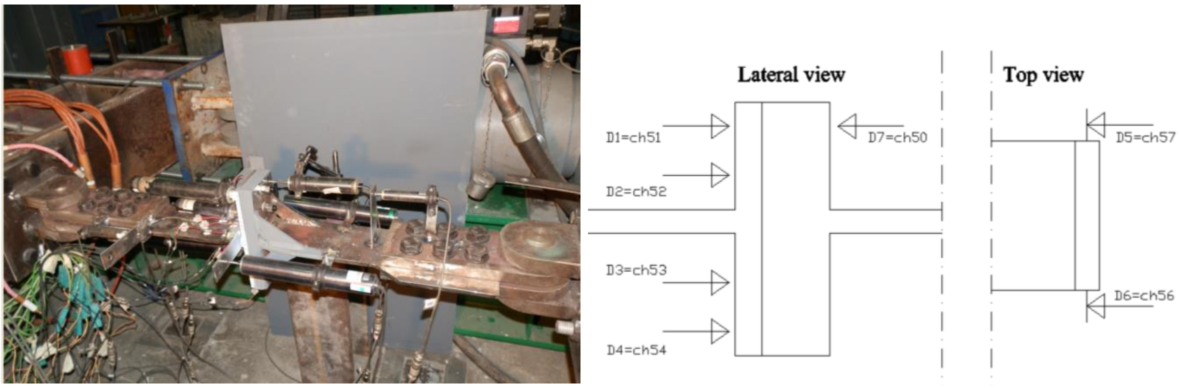


**Fig.** 7– Experimental setup and position of the instruments

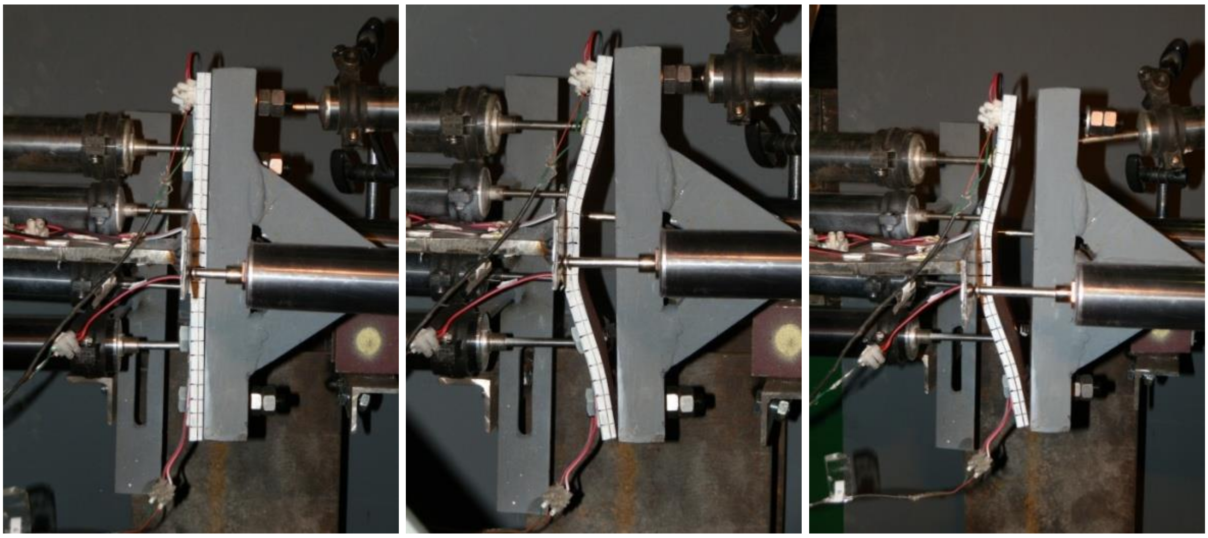

**Fig. 8–** Test 1 – Loading Sequence

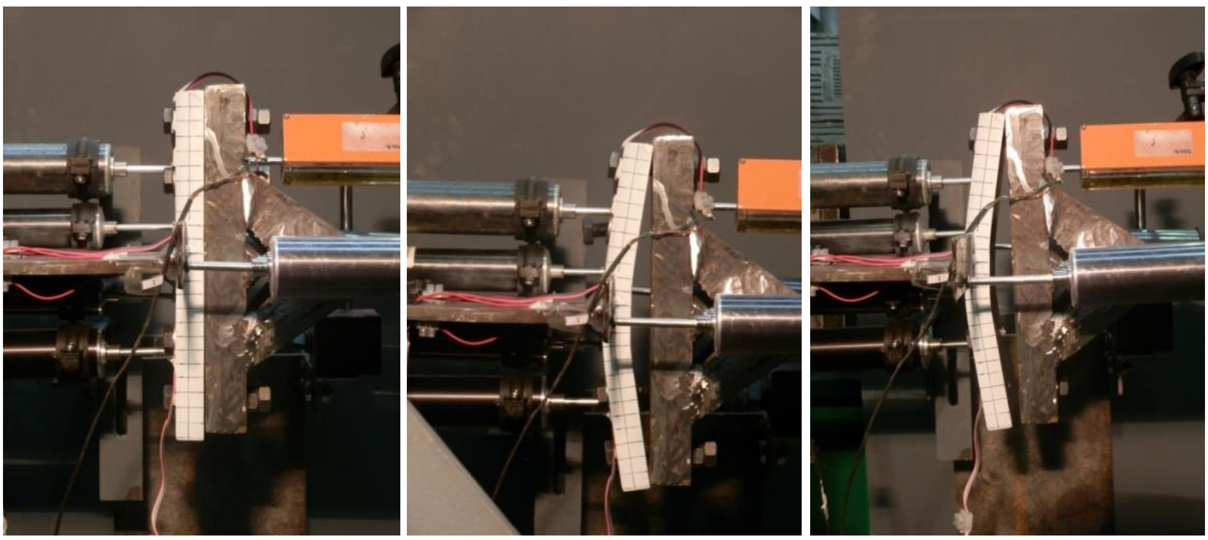

**Fig. 9–** Test 2 – Loading Sequence

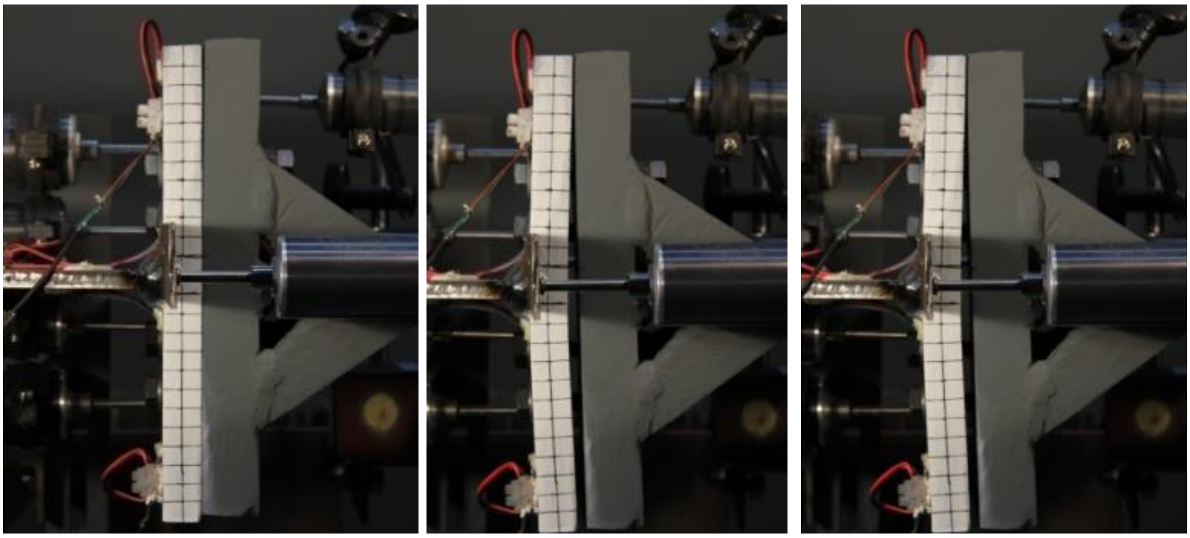

**Fig.10 –** Test 3 – Loading Sequence

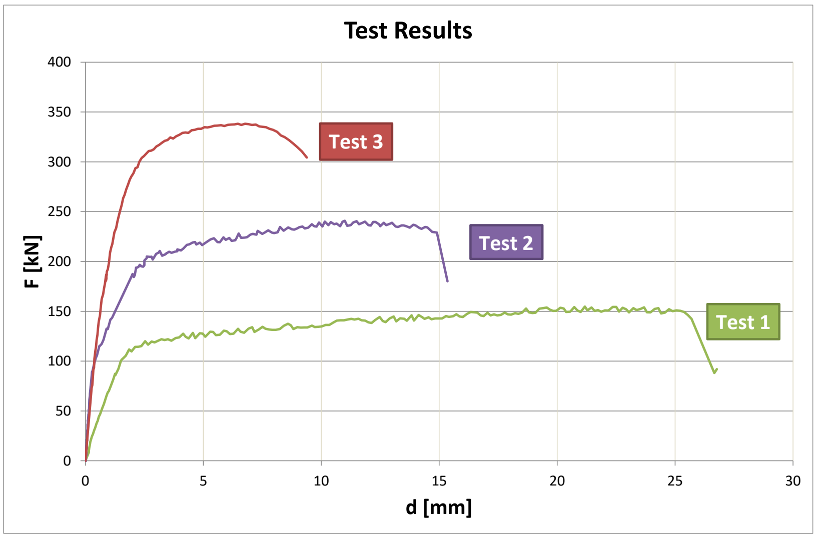


**Fig. 11 –** Experimental results of the tests

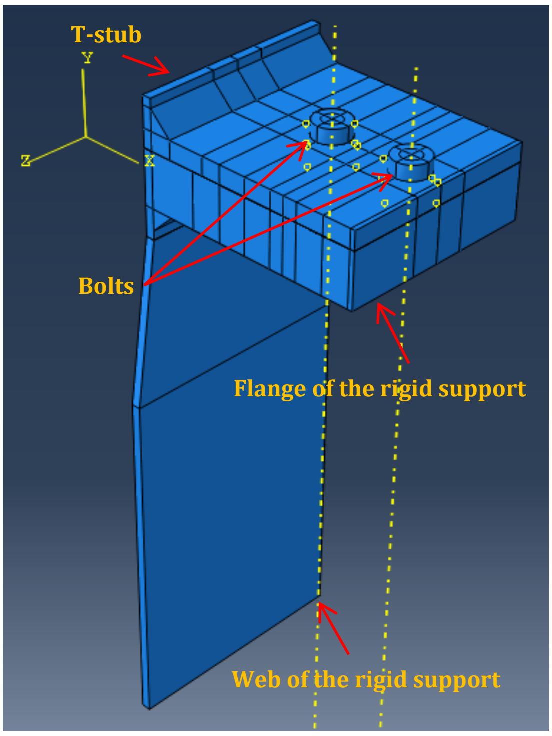


**Fig. 12 –**Developed FEM

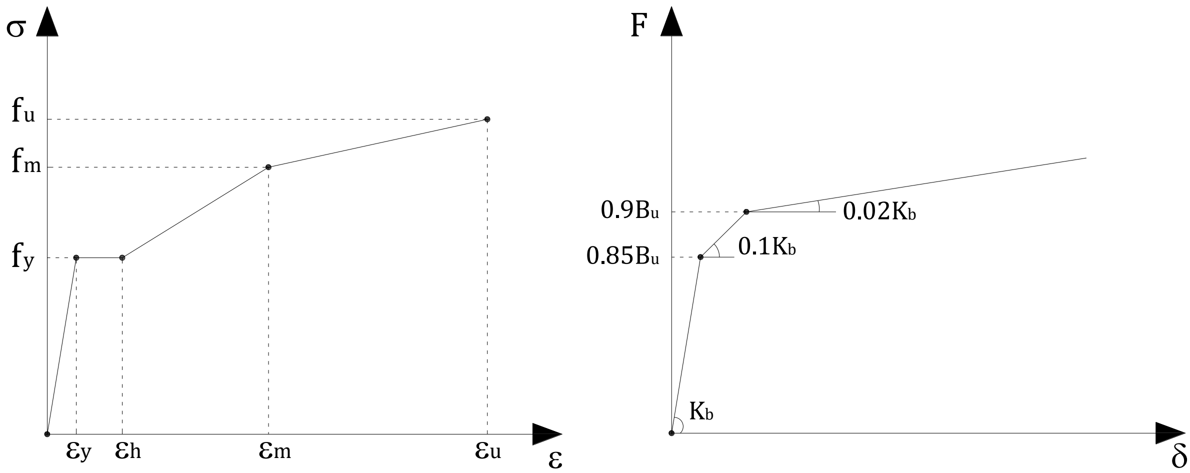


*a) Plate* *b) Bolt (Leon & Swanson,2000)*

**Fig. 13 –**Behaviour laws adopted in the simulation

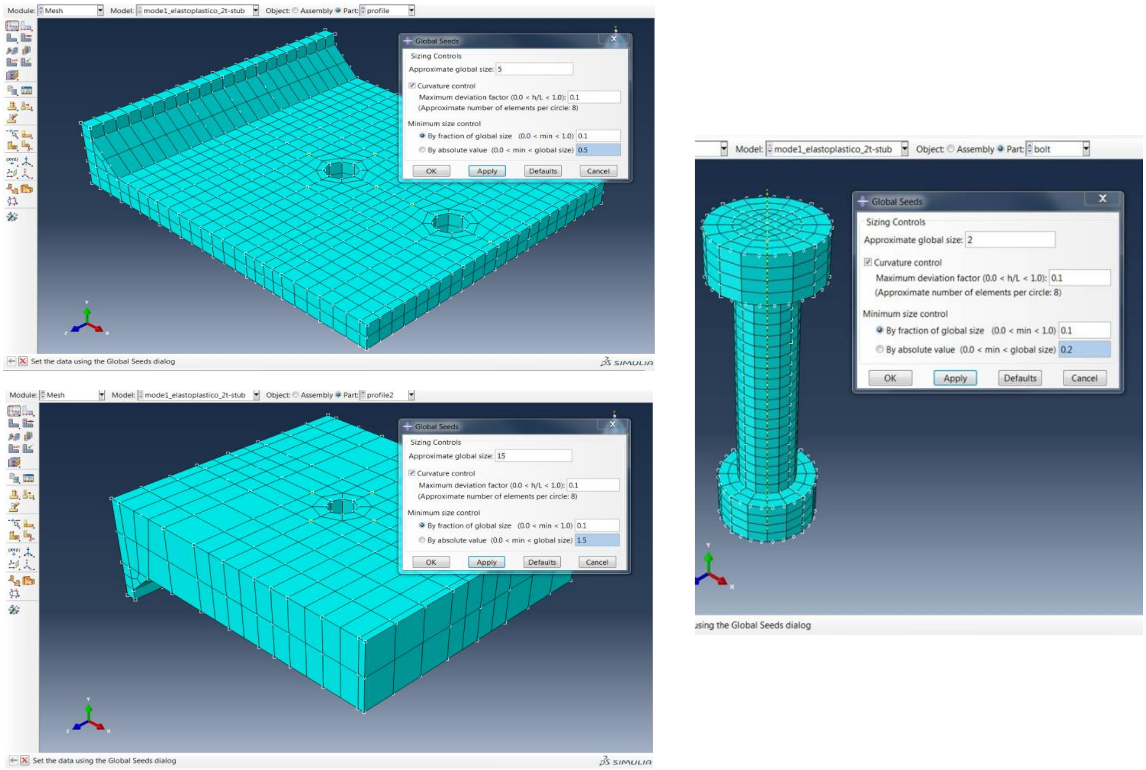


**Fig. 14 –**Mesh Size

a)

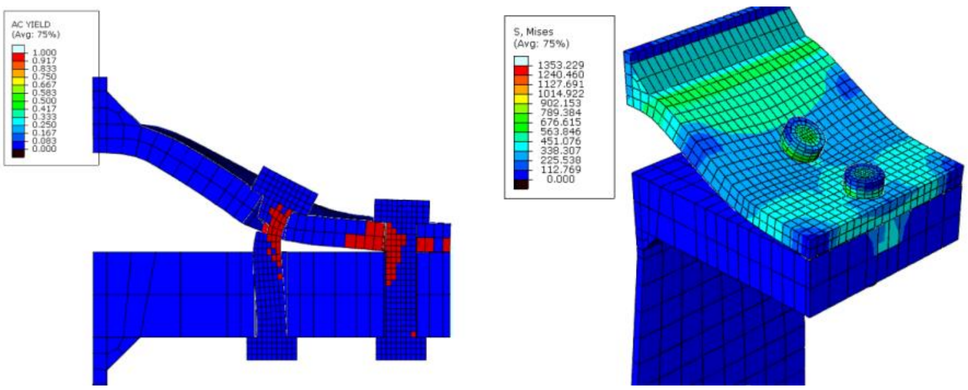


b)

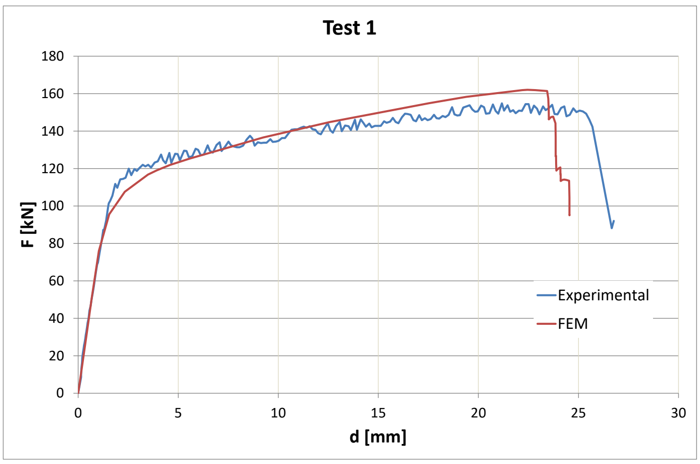


**Fig. 15 –** Results of Test-1: a) stress and yield state at failure; b) force-displacement

curve

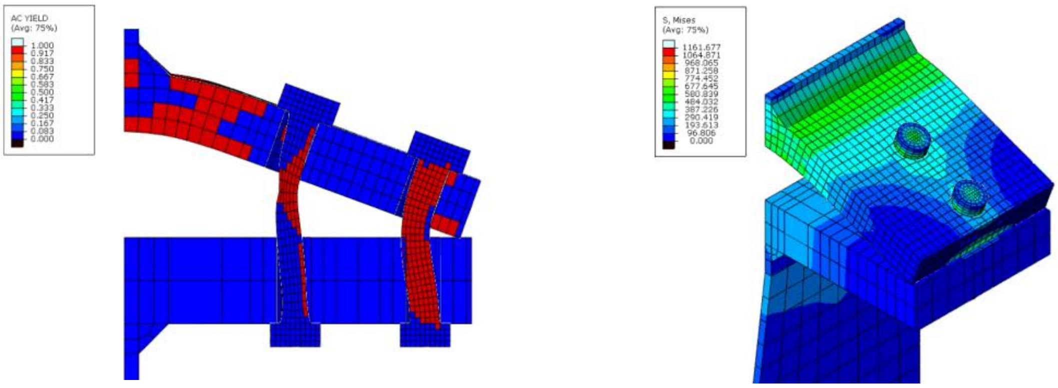


a)

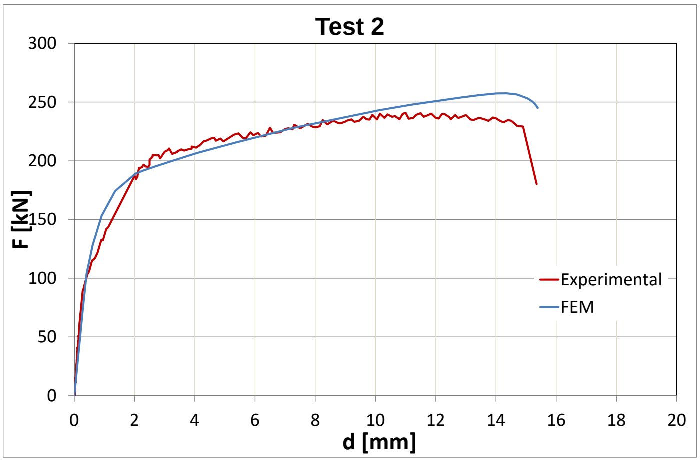


c)

**Fig. 16 –** Results of Test-2: a) stress and yield state at failure; b) force-displacement curve

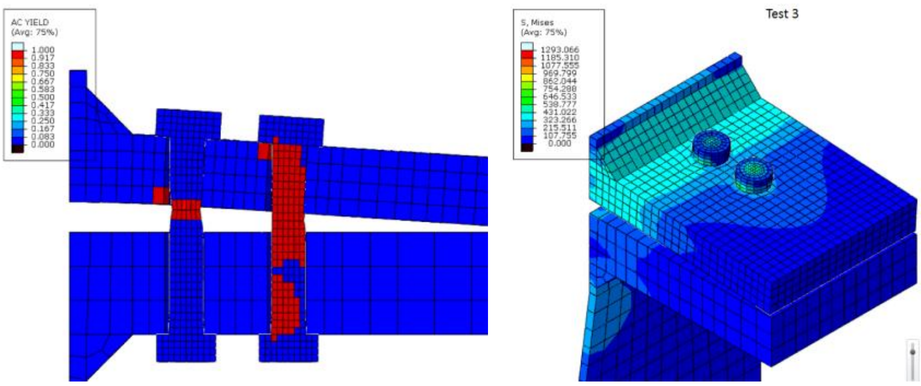


a)

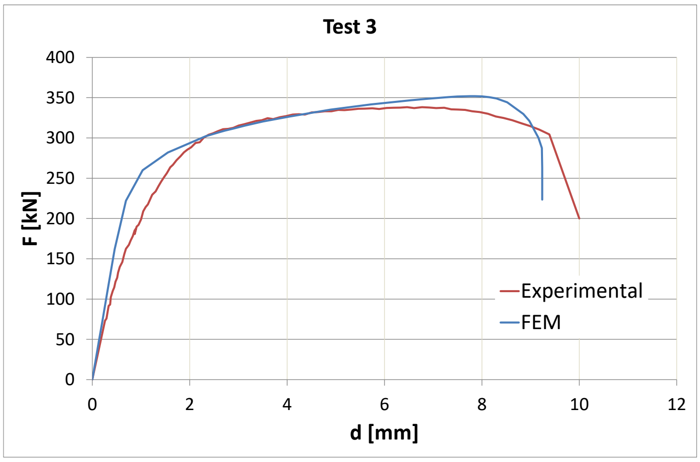


**b)**

**Fig. 17 –** Results of Test-3: a) stress and yield state at failure; b) force-displacement curve

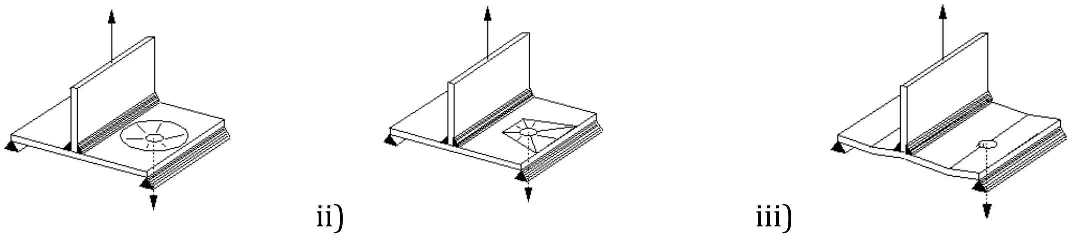

i) ii) iii)

**Fig. 18–** Failure modes of a T-stub with two bolts in one row: i) circular pattern, ii) non-circular pattern and iii) beam pattern.

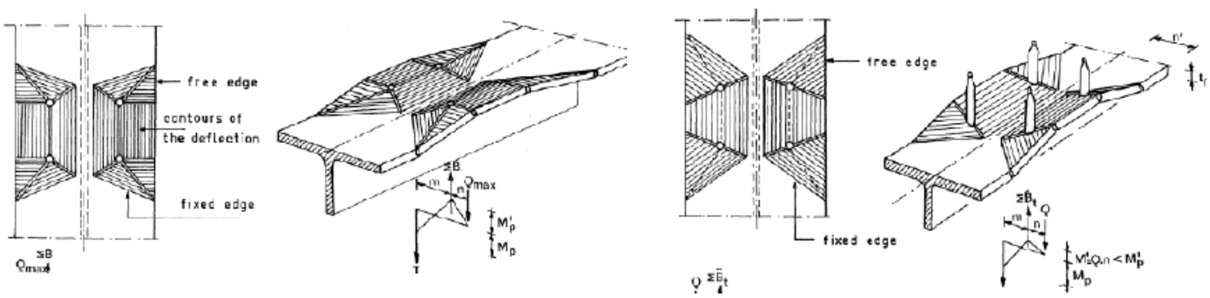


**a)** Mechanism type-1

**b)** Mechanism type-2

**Fig. 19 –** Classical non-linear patterns arising in two-bolts T-stub (Zoetemeijer, 1974)

| T-stub with 2-bolts | T-stub with 4-bolts |
| --- | --- |
| 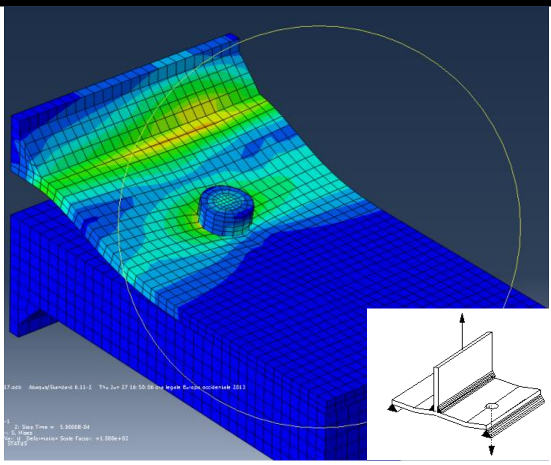 | 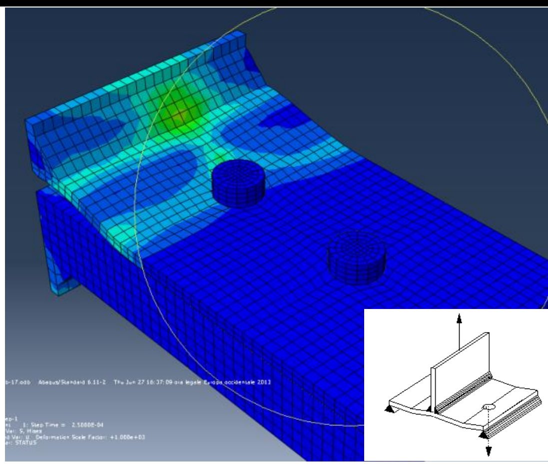 |
| ***Mec-1 - Beam Pattern*** | *Mec-1 - Beam Pattern* |
| 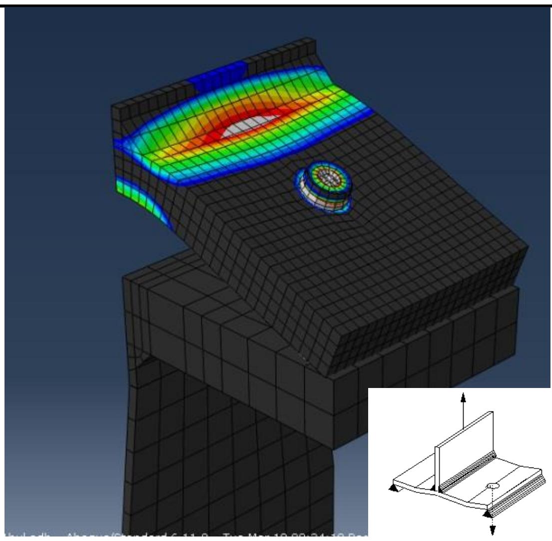 | 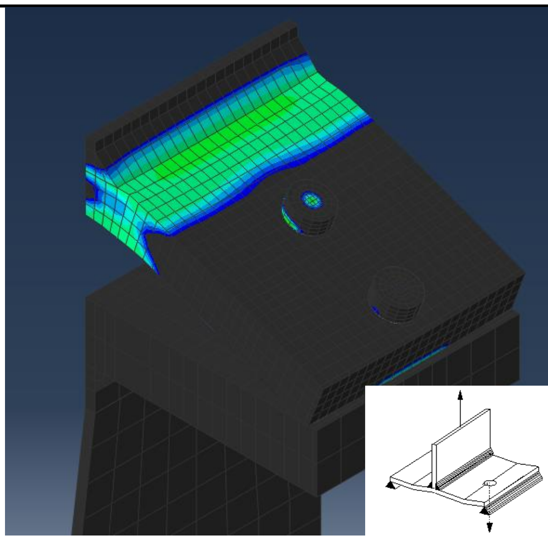 |
| *Mec-2 - Beam Pattern* | *Mec-2 - Beam Pattern* |
| 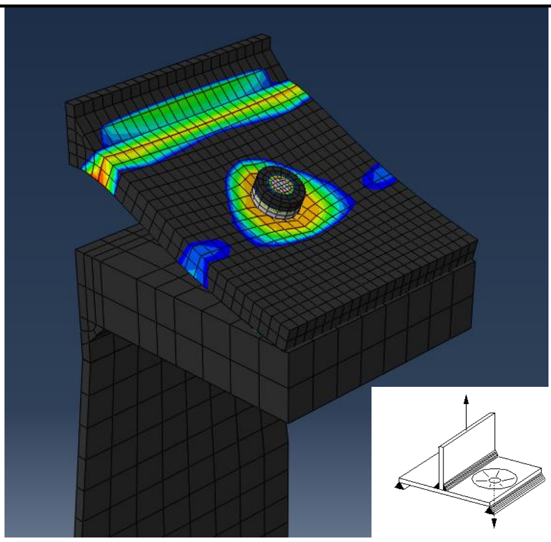 | 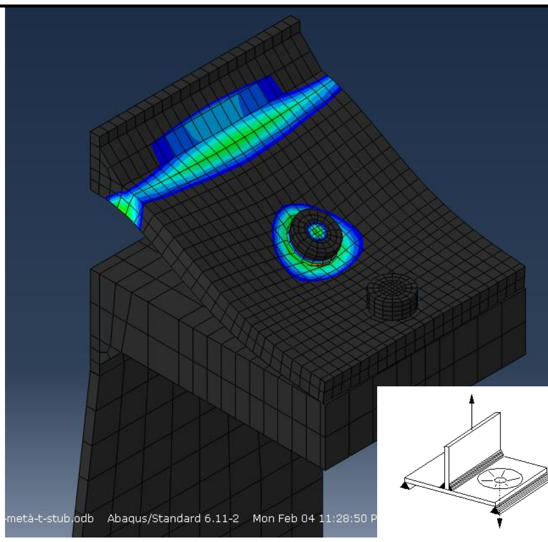 |
| | |

| T-stub with 2-bolts | T-stub with 4-bolts |
|---|---|
| *Mec-1 - Circular Pattern* | *Mec-1 - Circular Pattern* |

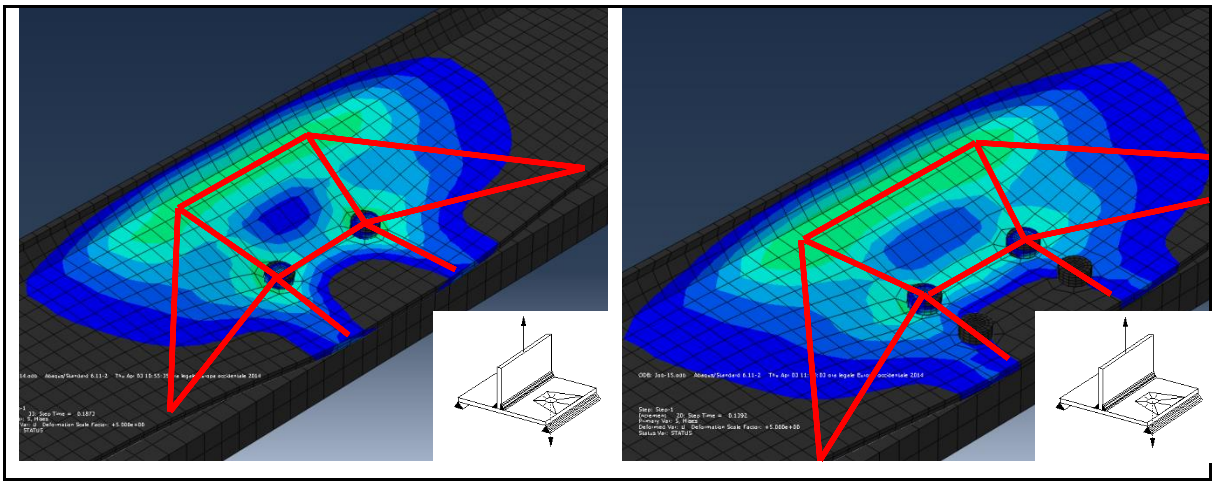

| | |
|---|---|
| *Mec-1 – Non-Circular Pattern* | *Mec-1 – Non-Circular Pattern* |

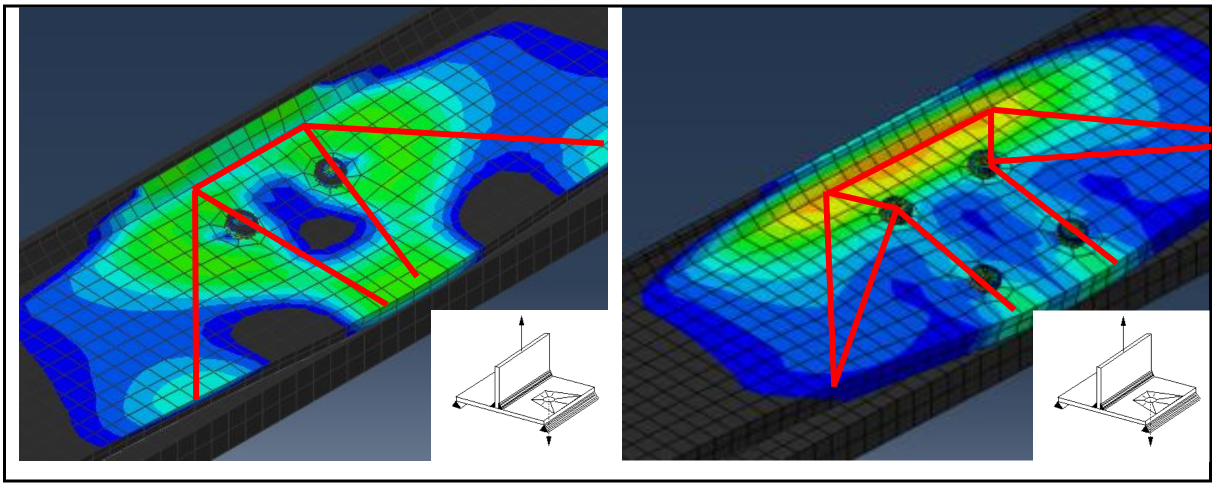

| | |
|---|---|
| *Mec-2 – Non-Circular Pattern* | *Mec-2 – Non-Circular Pattern* |

**Fig. 20 –** Yield linear patterns from FEM

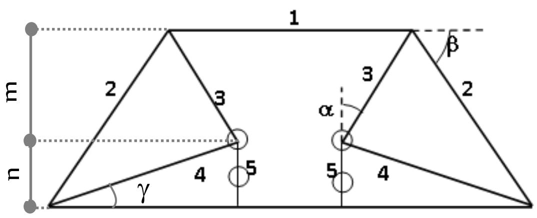


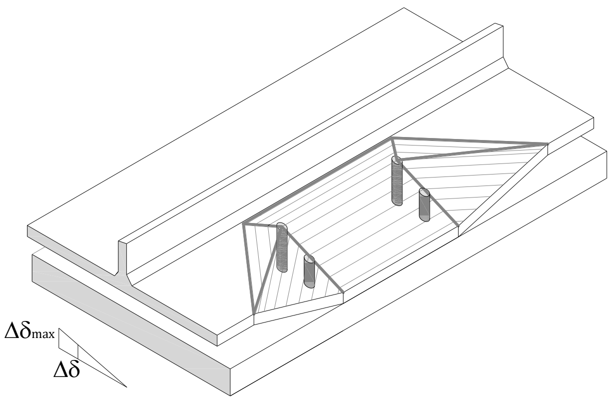

a) b)

**Fig. 21 –** Assumed yield line pattern: a) 2D idealization ; b) 3D idealization

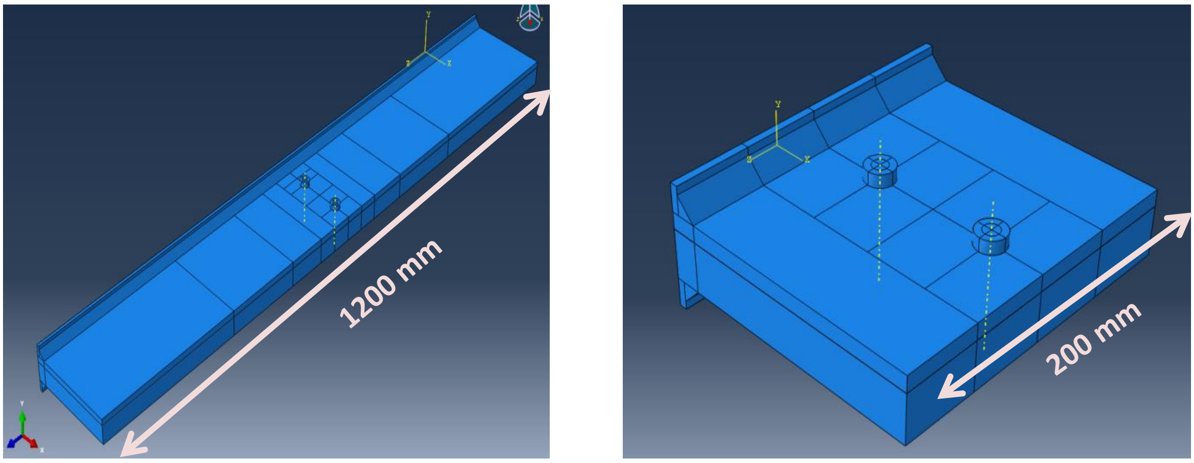


**Fig. 22 –** Cases generated in the parametric analysis

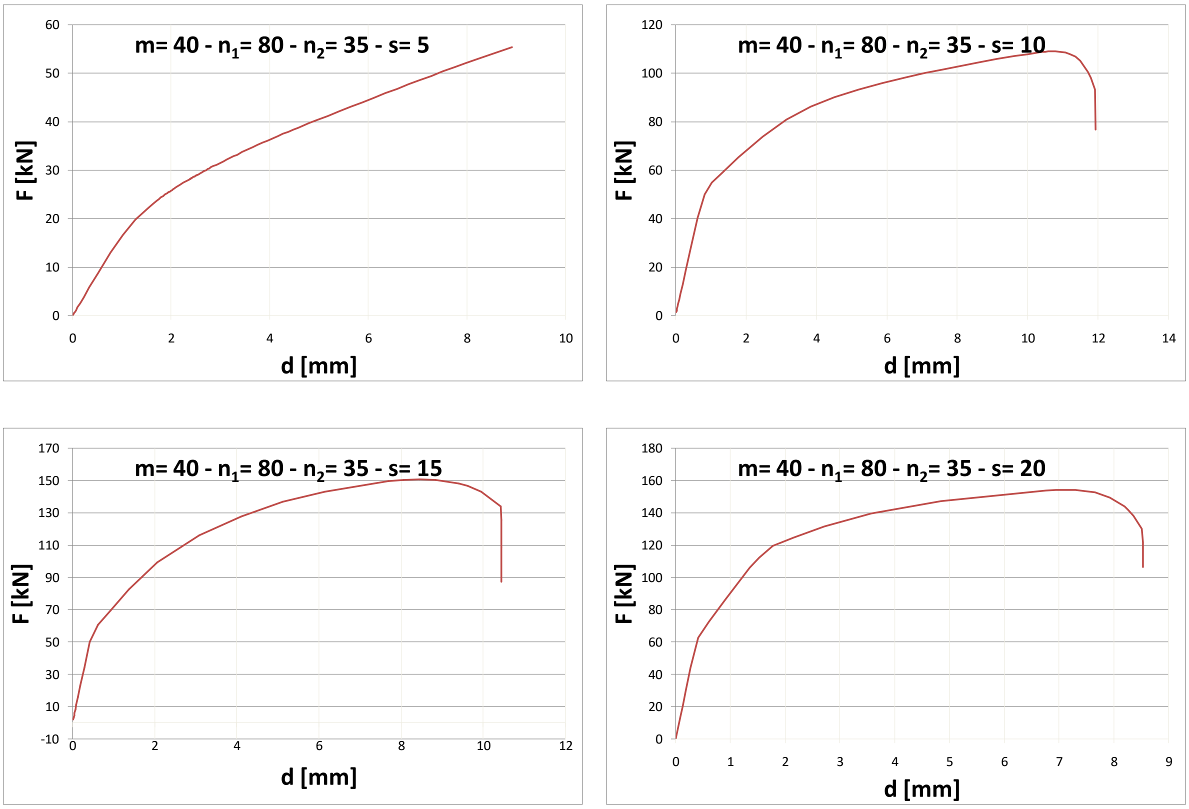


**Fig. 23 –** Some Cases Generated in the Parametric analysis

**Table 1** – Resistance of T-stubs with four bolts per row (Demonceau et al., 2010)

| Failure Mode | T-stub with two bolts | T-stub with 4 bolts |
|---|---|---|
| ***Mode-1*** | $F_1 = \frac{(8n - 2e_w)M_{pl,1,Rd}}{2mn - e_w(m+n)}$ | $F_1 = \frac{(8n - 2e_w)M_{pl,1,Rd}}{2mn - e_w(m+n)}$ |
| ***Mode-2*** | $F_2 = \frac{2M_{pl,2,Rd} + n\sum B_{t,Rd}}{(m+n)}$ | $F_2 = 2M_{pl,2,Rd} + \frac{\sum B_{t,Rd}}{2}\left(\frac{n_1^2 + 2n_2^2 + n_1 n_2}{n_1 + n_2}\right)$ |
| ***Mode-3*** | $F_3 = \sum B_{t,Rd}$ | $F_3 = \sum B_{t,Rd}$ |

**Table 2** – Geometrical Properties of the Specimens

| Specimen | $t_f$ [mm] | $t_w$ [mm] | B [mm] | L [mm] | d [mm] | $n_1$ [mm] | $n_2$ [mm] |
|---|---|---|---|---|---|---|---|
| **Test-1** | 10 | 10 | 105 | 250 | 46 | 46 | 18 |
| **Test-2** | 20 | 10 | 105 | 250 | 46 | 46 | 18 |
| **Test-3** | 20 | 10 | 105 | 250 | 17 | 29 | 64 |

where: $t_f$ and $t_w$ are the flange and web thickness of the T-stub, respectively; B is the T-stub width; L is the T-stub length; d is distance of the bolt from the web; $n_1$ and $n_2$ are illustrated in Fig.3.

**Table 3** – Materials Mechanical Properties

| Specimen | $f_y$ [MPa] | $f_m$ [MPa] | $f_u$ [MPa] | $\varepsilon_y$ [%] | $\varepsilon_h$ [%] | $\varepsilon_m$ [%] | $\varepsilon_u$ [%] |
|---|---|---|---|---|---|---|---|
| **Plate 10 mm** | 413 | 686 | 1075 | 0.20 | 1.70 | 10.36 | 81 |
| **Plate 20 mm** | 380 | 610 | 1018 | 0.18 | 1.40 | 6.78 | 81 |

the notation adopted for the symbols is reported in Fig.13

**Table 4** – Model vs FEM

| B [mm] | s [mm] | m [mm] | $n_1$ [mm] | $n_2$ [mm] | $l_{eff}$ [mm] | MEC | YLP | $F_{t,rd,MOD}$ [kN] | $F_{t,rd,FEM}$ [kN] | Ratio |
|---|---|---|---|---|---|---|---|---|---|---|
| 1200 | 5 | 40 | 80 | 35 | 251.2 | 1 | CP | 27.87 | 33.37 | 0.83 |
| 1200 | 5 | 60 | 60 | 35 | 358.75 | 1 | NCP | 26.53 | 27.03 | 0.98 |
| 1200 | 5 | 40 | 60 | 55 | 251.2 | 1 | CP | 27.87 | 32.51 | 0.85 |
| 1200 | 10 | 40 | 80 | 35 | 906.5 | 2 | NCP | 91.43 | 80.27 | 1.13 |
| 1200 | 10 | 60 | 60 | 35 | 902.5 | 2 | NCP | 85.15 | 74.06 | 1.14 |

| B [mm] | s [mm] | m [mm] | $n_1$ [mm] | $n_2$ [mm] | $l_{eff}$ [mm] | MEC | YLP | $F_{t,rd,MOD}$ [kN] | $F_{t,rd,FEM}$ [kN] | Ratio |
|---|---|---|---|---|---|---|---|---|---|---|
| 1200 | 10 | 40 | 60 | 55 | 906.5 | 2 | NCP | 95.84 | 79.47 | 1.20 |
| 1200 | 15 | 40 | 80 | 35 | 906.5 | 3 | | 108.86 | 88 | 1.23 |
| 1200 | 15 | 60 | 60 | 35 | 902.5 | 3 | | 108.86 | 88 | 1.23 |
| 1200 | 15 | 40 | 60 | 55 | 906.5 | 3 | | 108.86 | 94 | 1.15 |
| 1200 | 20 | 40 | 80 | 35 | 906.5 | 3 | | 108.86 | 101 | 1.07 |
| 1200 | 20 | 60 | 60 | 35 | 902.5 | 3 | | 108.86 | 102 | 1.07 |
| 1200 | 20 | 40 | 60 | 55 | 906.5 | 3 | | 108.86 | 114 | 0.95 |
| 200 | 5 | 40 | 80 | 35 | 200 | 1 | BP | 22.19 | 29.17 | 0.76 |
| 200 | 5 | 60 | 60 | 35 | 200 | 1 | BP | 17.35 | 24.17 | 0.71 |
| 200 | 5 | 40 | 60 | 55 | 200 | 1 | BP | 22.19 | 30.74 | 0.72 |
| 200 | 10 | 40 | 80 | 35 | 200 | 1 | BP | 88.75 | 74.32 | 1.19 |
| 200 | 10 | 60 | 60 | 35 | 200 | 1 | BP | 59.17 | 67.34 | 0.87 |
| 200 | 10 | 40 | 60 | 55 | 200 | 1 | BP | 88.75 | 74.38 | 1.19 |
| 200 | 15 | 40 | 80 | 35 | 200 | 3 | | 108.86 | 83.05 | 1.31 |
| 200 | 15 | 60 | 60 | 35 | 200 | 3 | | 108.86 | 76.9 | 1.41 |
| 200 | 15 | 40 | 60 | 55 | 200 | 3 | | 108.86 | 86.67 | 1.25 |
| 200 | 20 | 40 | 80 | 35 | 200 | 3 | | 108.86 | 90.53 | 1.20 |
| 200 | 20 | 60 | 60 | 35 | 200 | 3 | | 108.86 | 87.48 | 1.24 |
| 200 | 20 | 40 | 60 | 55 | 200 | 3 | | 108.86 | 101.13 | 1.08 |
| | | | | | | | | | **Average** | 1.078 |
| | | | | | | | | | **ST.DEV** | 0.19 |